

Reward Breaks Through Center-Surround Inhibition via Anterior Insula

Lihui Wang,¹ Hongbo Yu,¹ Jie Hu,¹ Jan Theeuwes,² Xiaoliang Gong,³
Yang Xiang,³ Changjun Jiang,³ and Xiaolin Zhou^{1,4,5,6*}

¹Center for Brain and Cognitive Sciences and Department of Psychology, Peking University, Beijing, China

²Department of Experimental and Applied Psychology, Vrije Universiteit, Amsterdam, 1081 BT, The Netherlands

³Key Laboratory of Embedded System and Service Computing (Ministry of Education), Tongji University, Shanghai 201804, China

⁴Beijing Key Laboratory of Behavior and Mental Health, Peking University, Beijing 100871, China

⁵Key Laboratory of Machine Perception (Ministry of Education), Peking University, Beijing 100871, China

⁶PKU-IDG/McGovern Institute for Brain Research, Peking University, Beijing 100871, China

Abstract: Feedback inhibition is a fundamental neural mechanism that regulates the activity of neurons and neural circuits. It is thought to play a critical role in the generation of rhythmic oscillations and in the control of neural excitability. In this study, we investigated the role of the anterior insula (AI) in the generation of reward breaks through center-surround inhibition via AI. We used functional magnetic resonance imaging (fMRI) to measure brain activity during a task that required participants to respond to a reward signal. The results showed that the AI was activated during the reward phase of the task, and this activation was associated with the generation of reward breaks. These findings suggest that the AI plays a key role in the generation of reward breaks through center-surround inhibition via AI.

Conflict of interest statement: No potential conflict of interest was declared by the authors.
Correspondence to: Xiaolin Zhou, P.D., Department of Psychology, Peking University, Beijing, 100871, China.
E-mail: zhouxl@pku.edu.cn
Received 14 September 2015; Accepted 17 September 2015
Published online 29 September 2015 in Wiley Online Library (wileyonlinelibrary.com). DOI: 10.1002/hbm.23004
© 2015 Wiley Periodicals, Inc.

... AI ... *Hum Brain Mapp* 36:5233–5251, 2015. © 2015 Wiley Periodicals, Inc.

Key words: ... fMRI;

INTRODUCTION

I ...

S ...

A ...

J ...

T ...

F ...

A ...

O ...

A ...

(VS) ...

K ...

B ...

I ... fMRI

... C ... T ... 2003; M ... 2000 .

W ...

I ...

W ... 2014 . S ...

I ...

A ... 2011 . M ...

E ... W ...

(0.9°) ...

(2.1 ... 4.5°),

(0.9° ... 2.1°) W ... 2014 . A ...

2000 , e ...

1.54°

(0.9°) ...

(1.6/2.8/4.0°)

W ...

(1.6°),

(2.8/4.0°).

T ...

IPS,

Le ... S ... 1999;

P ... G ... 1999 . H ...

M ... 2004 . T ...

W ...

f ...

200 EPI volumes, resulting in 300 volumes (echo time = 30 ms, echo spacing = 3.75 ms, TR = 1200 ms, TE = 30 ms, TE_{eff} = 23.25 ms). The data were processed using SPM8 (Wellcome Trust Centre for Neuroimaging, London, UK). Functional images were slice-timed and coregistered to T1-weighted anatomical images using SPM8. Images were then normalized to MNI space using a 3 × 3 × 3 mm³ grid. The resulting images were smoothed with a Gaussian kernel of 6 mm FWHM.

Task fMRI data

Data were processed using SPM8 (Wellcome Trust Centre for Neuroimaging, London, UK). Functional images were slice-timed and coregistered to T1-weighted anatomical images using SPM8. Images were then normalized to MNI space using a 3 × 3 × 3 mm³ grid. The resulting images were smoothed with a Gaussian kernel of 6 mm FWHM.

Resting-state fMRI data

Resting-state data were processed using SPM8. Data were processed using the DPARSF toolbox (Ding et al., 2010). Functional images were slice-timed and coregistered to T1-weighted anatomical images using SPM8. Images were then normalized to MNI space using a 3 × 3 × 3 mm³ grid. The resulting images were smoothed with a Gaussian kernel of 6 mm FWHM.

Statistical Analysis of Behavioral Data

Behavioral data were analyzed using a two-sample t-test. Reaction times (RT) were analyzed using a two-sample t-test. Mean RT was 800 ms (95.1% CI: 780-820 ms). The difference between conditions was significant ($t = 2.34$, $p = 0.02$). We used $\alpha = 0.05$. The null hypothesis was that there is no difference between conditions ($H_0: \mu_1 = \mu_2$). The alternative hypothesis was that there is a difference ($H_1: \mu_1 \neq \mu_2$). We used a two-tailed test. The test statistic was $t = 2.34$. The p-value was 0.02. We reject the null hypothesis. The results are significant.

Statistical Analysis of Imaging Data

Whole-brain analysis

The whole-brain analysis was performed using SPM8. The data were analyzed using a two-sample t-test. The results are shown in Figure 1. The significant clusters are located in the left inferior parietal lobule (LIP), left inferior frontal gyrus (LIFG), and left superior frontal gyrus (LSFG). The coordinates are: LIP (x = -45, y = -60, z = 15), LIFG (x = -45, y = 15, z = 15), and LSFG (x = -15, y = 15, z = 30). The p-values are: LIP ($p = 0.001$), LIFG ($p = 0.001$), and LSFG ($p = 0.001$). We used a two-tailed test. The test statistic was $t = 3.45$. The p-value was 0.001. We reject the null hypothesis. The results are significant.

TABLE II. Brain areas revealed in the test phase

Region	Hemisphere	BA	MNI			t	Cluster size
			x	y	z		
H1 > Me (H2 + H3)							
IPS	L	7	-27	-67	46	6.01	514
LOC	L	37	-45	-64	-11	4.86	92
IFG (Tri.)	R	45	48	29	19	4.34	57
MOG	L	19	-36	-85	16	4.11	48
MFG	R	6	30	8	49	4.00	91
IFG	L	44	-51	11	31	3.94	213
IPS	R	19	30	-61	34	3.69	177
IFG (Oper.)	R	44	48	11	22	3.65	48
H1 > L1							
LOC	L	37	-48	-64	-11	6.56	225
IPS	L	40	-36	-46	55	5.45	284
MOG	L	19	-33	-82	19	4.50	112
LOC	R	20	48	-43	-26	4.13	52
SMA	L	32	-9	14	43	4.02	51
PI	L	48	-36	-22	10	4.01	161
IFG	L	44	-51	11	34	3.98	283
AI	R	47	27	23	-14	3.75	107
AI	L	48	-27	20	-5	3.64	41
IPS	R	7	27	-46	43	3.58	58
H1 > Me (H2 + H3) ∩ H1 > L1							
IPS	L	40	-39	-43	55	4.93	290
LOC	L	37	-45	-64	-11	4.86	78
MOG	L	19	-33	-88	16	3.90	39
IFG	L	44	-51	11	34	3.56	98
H1 > H2 (e.g., H1 > Me (H2 + H3))							
LOC	L	19	-39	-82	-8	4.53	97
LOC	R	41	48	-43	26	4.13	52
SMA	L	32	-9	14	43	4.02	50
PI	L	48	-36	-22	10	4.01	160
PCG	L	6	-54	-4	43	3.98	174
MOG	L	18	-27	-88	19	3.90	50
AI	R	48	27	17	-14	3.86	67
AI	L	48	-27	20	-5	3.64	41
Me (H2 + H3) > H1							
PCC	L/R	23	0	-46	19	4.31	156
Pe	R	7	3	-76	37	4.29	106
L1 > H1							
Pe	R	23	3	-40	28	3.49	52

Note: AI: anterior insular cortex; BA: Brodmann area; IFG: inferior frontal gyrus; IPS: inferior parietal lobule; LOC: lateral occipital cortex; MFG: middle frontal gyrus; MOG: middle occipital gyrus; Oper.: opercular part; PCC: posterior cingulate cortex; PCG: precentral gyrus; PI: pre-
 T.: transverse.

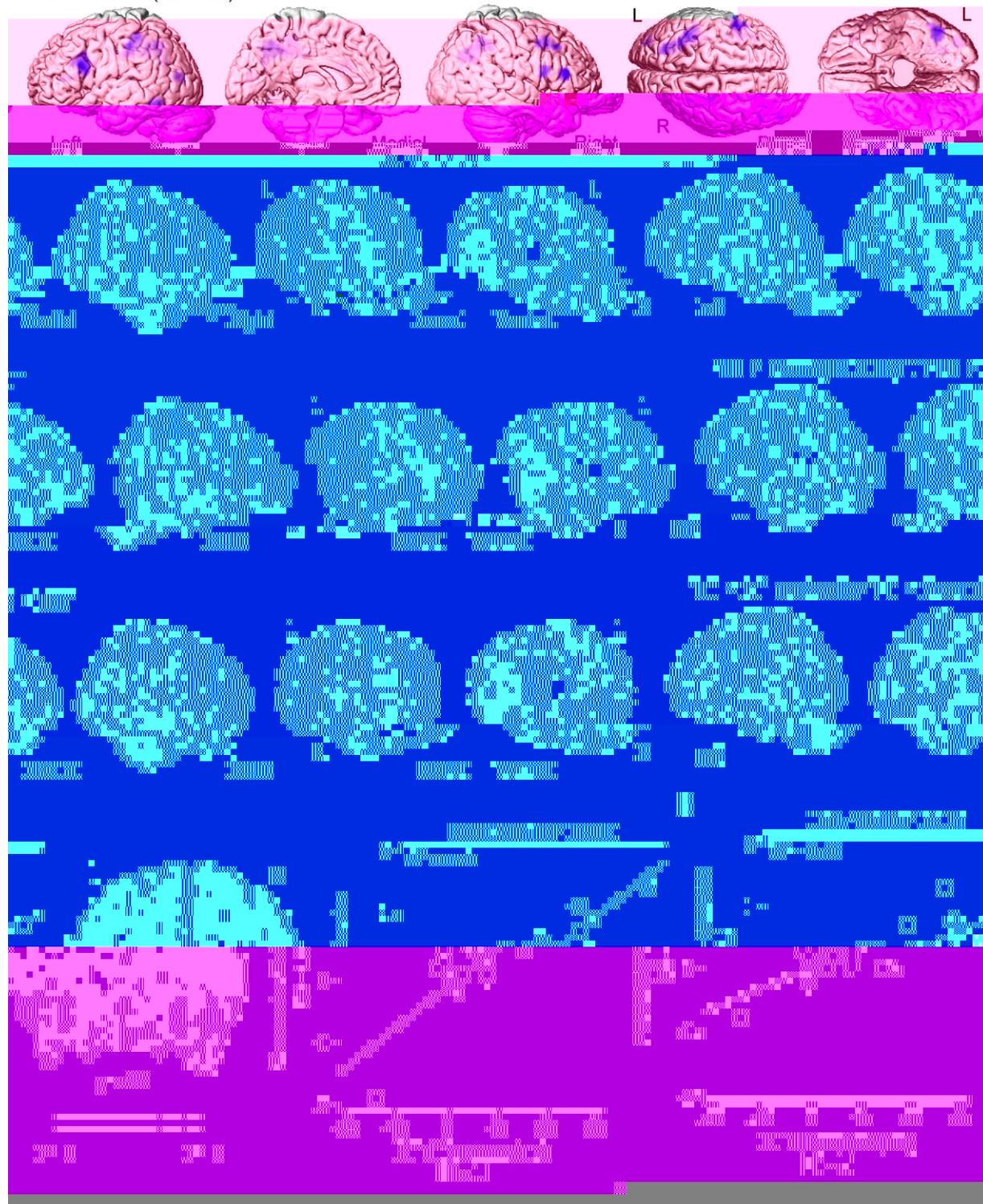
... The ...
 ...
 ... ANOVA ...
 ... SPM8 ...
 ...

...
 ... SPM8. We ...
 ... H1 > L1 ... H1 > Me (H2 + H3). The ...
 ...
 ... H1 > L1 ...
 ... (e.g., RT ... H1 ... RT ...
 ... L1) ...
 ... AFNI ... A ... S ...
 ...
 ... 6 ... 3 FWHM. A ...
 ...
 ... (FWE)- ...
 ... 35 ...
 ... P < 0.005 ...
 ... (...) ...
 ... C ... , 2009 .

Region of interest (ROI) analysis

A ...
 ... A ... , 2013 , ...
 ...
 ...
 ... D ... , 1995; L ... , 1997 . E ...
 ...
 ...
 ... B ... , 2009; H ... , 2006 . We ...
 ...
 ... We ...
 ... S ... , e ...
 ...
 ... (e.g., ... - ...) .
 ...
 ...
 ... P < 0.05 FWE- ...
 ... A ...
 ... (BA19, F ... 2B). The ...
 ... GLM ...
 ... GLM ...
 ...
 ... (e.g., ...) ...
 ... P ...
 ...
 ...
 ... (e.g., x = -36, y = -88, z = 16; ... : x = 39, y = -76, z = -14). The ...
 ...
 ...
 ... 2 (He ... : e ...) ×
 ... 2 (Re ...) × 3 (L ... : 1, 2 ... 3) ANOVA ...
 ...

A "H1 > Mean (H2 + H3)"



Dynamic causal modeling

Dynamic causal modeling (DCM) is a Bayesian framework for modeling the time course of neural activity in response to an external input. In this study, we used DCM10 (Friston et al., 2003) to model the data. The model structure was defined by the connectivity matrix (Table III). We estimated the model parameters for each subject using variational Bayes (Friston et al., 2008). The model was fitted to the data using the Expectation-Maximization algorithm (Friston et al., 2003). The model was then used to generate predictions of the data. The model was fitted to the data using the Expectation-Maximization algorithm (Friston et al., 2003). The model was then used to generate predictions of the data. The model was fitted to the data using the Expectation-Maximization algorithm (Friston et al., 2003). The model was then used to generate predictions of the data. The model was fitted to the data using the Expectation-Maximization algorithm (Friston et al., 2003). The model was then used to generate predictions of the data.

TABLE III. The structures of the modulatory connectivity in DCM

Modulatory connectivity	1	2	3	4	5	6	7	8	9
AI → IFG	1	1	0	0	0	0	1	1	0
AI → IPS	1	1	0	1	1	0	0	0	0
IFG → LOC	1	0	1	0	0	0	1	0	1
IPS → LOC	1	0	1	1	0	1	0	0	0

Notes: AI: Anterior Insular Cortex; IFG: Inferior Frontal Gyrus; IPS: Intraparietal Sulcus; LOC: Lateral Occipital Cortex; 1: excitatory, 0: inhibitory.

Results of the whole brain analysis for the test phase. **A:** Blue: the activations revealed by the contrast “H1 > Mean (H2 + H3)”. Red: the activations revealed by the contrast “H1 > L1.” Purple: the common activated regions of the two networks. Green: the brain activations revealed by the contrast “H1 > L1” exclusively masked by the contrast “H1 > Mean (H2 + H3)”. Statistical parametric map was shown at the threshold of $P < 0.005$ FWE-corrected at cluster level, $P < 0.005$ uncorrected at voxel level (H1: high-reward distractor, location 1; H2: high-reward distractor, location 2; H3: high-reward distractor, location 3; L1: low-reward distractor, location 1). **B:** AI was activated by the contrast “H1 > L1” when the RT difference between H1 and L1 conditions were included as covariates

(middle panel). Parameter estimates were extracted from the two clusters. Scatter plots (with best-fitting regression lines) illustrates the difference of the parameter estimates between H1 and L1 conditions as a function of the RT difference (left and right panels). In the right panel, the correlation was still significant after the outlier (the bottom left dot) is excluded from the data ($R^2 = 0.59$). Thus, we keep all the data points in the plot. Note that the bottom left dot in the right panel was identified as the only outlier because the activity strength (the value of parameter estimates) of this dot in the right AI was beyond $-3SD$ of the group mean. No outlier was found in the left panel.

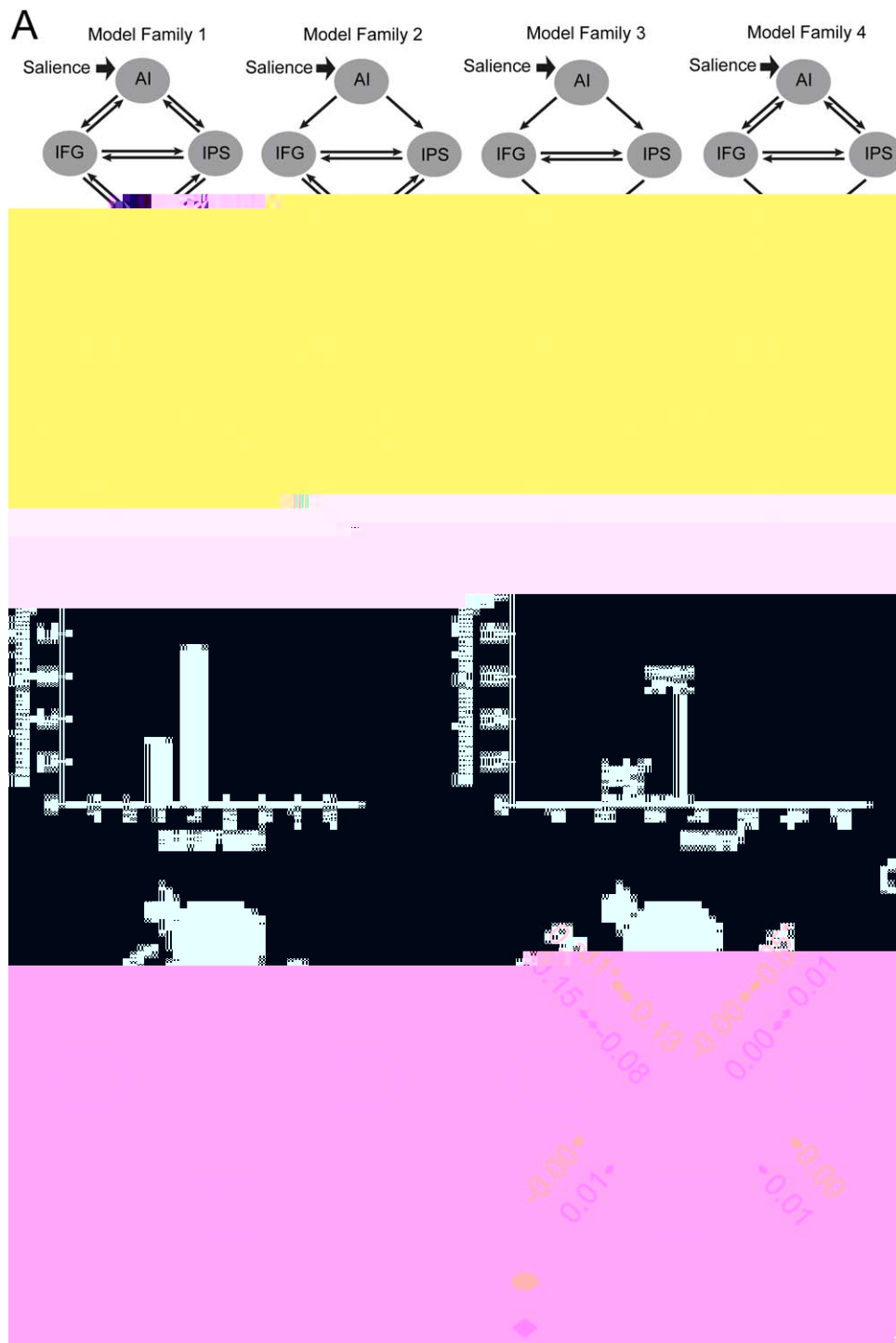


Figure 4.

The dynamic causal modeling (DCM) analysis for AI and the fronto-parietal network. **A:** The structure of 8 model families (left hemisphere). These model families differed in terms of the presence or absence of the intrinsic connectivity from LOC to AI, the direction of the intrinsic connectivity between AI and IFG/IPS, the direction of the intrinsic connectivity between IFG/IPS and LOC, and the input. Each model family contained nine models, which differed in the specific pathway(s) that modulated

by reward (HI vs. LI, see Table III). **B:** The exceedance probabilities of the eight model families (left panel) and the single models (right panel). The single models from the eight model families were ordered in consistency with Table III. **C:** The estimated DCM parameters of the average model of the winning family (* $P < 0.05$, ** $P < 0.01$, # $P = 0.051$). [Color figure can be viewed in the online issue, which is available at wileyonlinelibrary.com.]

Resting-state analysis

Analysis of resting-state functional connectivity (FC) revealed significant differences between the groups. The independent component (IC) analysis identified several components, including the default mode network (DMN), the dorsal attention network (DAN), and the ventral attention network (VAN). The FC analysis showed that the DAN and VAN were significantly more active in the H1 group compared to the H2 and H3 groups. The results are summarized in Table 1.

Table 1: Resting-state functional connectivity (FC) analysis results. The table shows the mean FC values for each component across the three groups (H1, H2, H3) and the corresponding statistical significance (P-value and 95% CI).

Component	H1 (Mean)	H2 (Mean)	H3 (Mean)	Statistical Significance
DMN	0.15	0.12	0.10	$P < 0.05$, 95% CI [0.05, 0.25]
DAN	0.25	0.18	0.15	$P < 0.01$, 95% CI [0.10, 0.40]
VAN	0.20	0.15	0.12	$P < 0.05$, 95% CI [0.05, 0.35]

RESULTS

Behavioral Data

Behavioral data were collected for each group. The results showed that the H1 group had significantly faster reaction times (RT) compared to the H2 and H3 groups. The statistical analysis revealed a significant main effect of group on RT, $F(2, 26) = 11.20, P < 0.001, \eta_p^2 = 0.463$. Post-hoc analysis showed that the H1 group was significantly faster than the H2 group, $F(1, 13) = 4.63, P < 0.05, \eta_p^2 = 0.263$, and the H3 group, $F(1, 13) = 11.74, P < 0.001, \eta_p^2 = 0.474$.

Behavioral data were collected for each group. The results showed that the H1 group had significantly faster reaction times (RT) compared to the H2 and H3 groups. The statistical analysis revealed a significant main effect of group on RT, $F(2, 26) = 11.20, P < 0.001, \eta_p^2 = 0.463$. Post-hoc analysis showed that the H1 group was significantly faster than the H2 group, $F(1, 13) = 4.63, P < 0.05, \eta_p^2 = 0.263$, and the H3 group, $F(1, 13) = 11.74, P < 0.001, \eta_p^2 = 0.474$.

Behavioral data were collected for each group. The results showed that the H1 group had significantly faster reaction times (RT) compared to the H2 and H3 groups. The statistical analysis revealed a significant main effect of group on RT, $F(2, 26) = 11.20, P < 0.001, \eta_p^2 = 0.463$. Post-hoc analysis showed that the H1 group was significantly faster than the H2 group, $F(1, 13) = 4.63, P < 0.05, \eta_p^2 = 0.263$, and the H3 group, $F(1, 13) = 11.74, P < 0.001, \eta_p^2 = 0.474$.

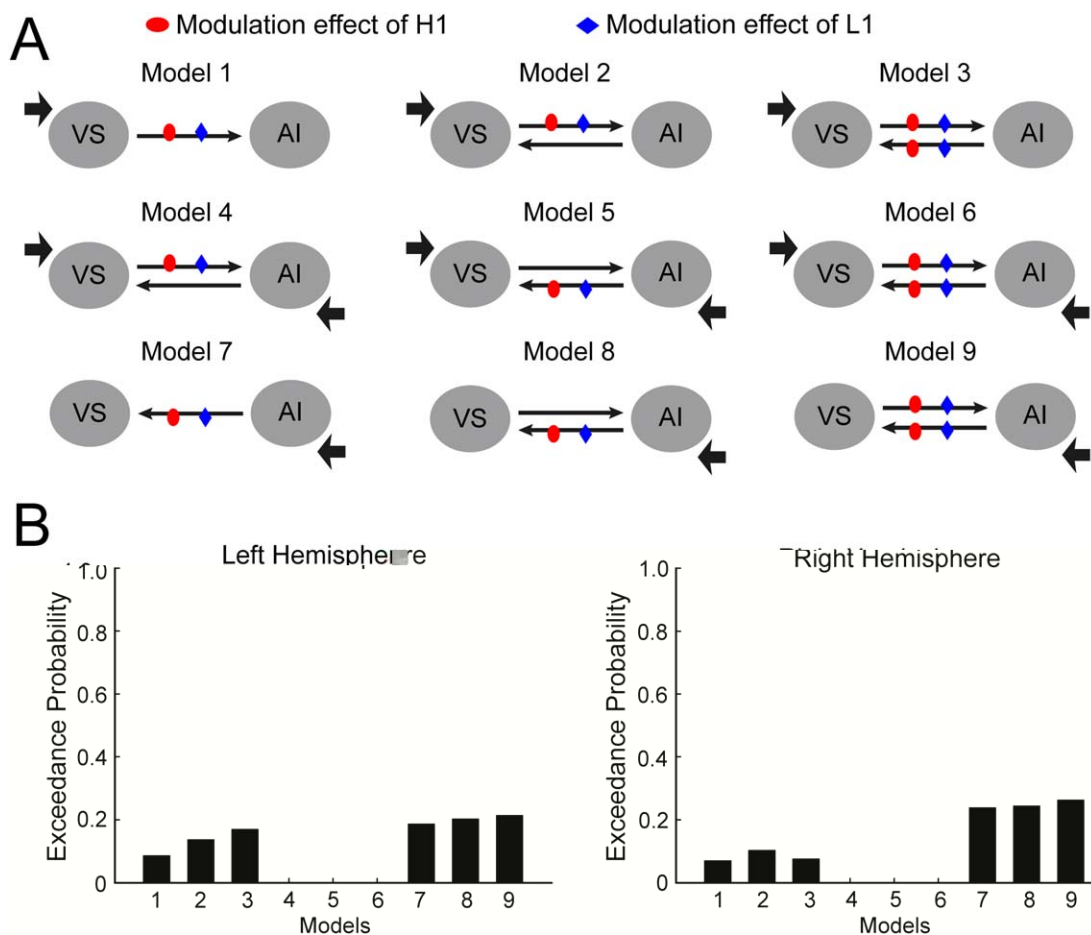


Figure 5.

The DCM analysis for AI and VS. **A:** The structure of 12 models with different intrinsic connectivities and modulatory connectivities. **B:** The exceedance probabilities of the 12 models in the left (left panel) and the right (right panel) hemisphere. [Color figure can be viewed in the online issue, which is available at wileyonlinelibrary.com.]

the effects of H2, H3, $P > 0.1$, 95% CI -7.7 , 10.5 ($F_{(1, 32)} = 1.1$, $P = 0.31$). For the effects of L1, L2, L3, $F_{(1, 32)} = 2.89$, $P < 0.05$, 95% CI 1.8 , 11.7 , $F_{(1, 32)} = 4.4$, $P < 0.05$, 95% CI -9.1 , 4.4 , $F_{(1, 32)} = 0.1$, $P > 0.1$, 95% CI -5.8 , 5.4 . ANOVA revealed significant effects of H1, $F_{(2, 64)} = 10.5$, $P < 0.001$, $\eta_p^2 = 0.279$.

We conducted a series of planned comparisons (i.e., $H1 > H2$, $H1 > H3$) to test the effects of H1 on RT, $F_{(1, 32)} = 10.5$, $P < 0.001$, $\eta_p^2 = 0.279$. We also conducted a series of planned comparisons to test the effects of L1, L2, and L3 on RT, $F_{(1, 32)} = 2.89$, $P < 0.05$, $\eta_p^2 = 0.082$; $F_{(1, 32)} = 4.4$, $P < 0.05$, $\eta_p^2 = 0.12$; $F_{(1, 32)} = 0.1$, $P > 0.1$, $\eta_p^2 = 0.003$. We also conducted a series of planned comparisons to test the effects of H1, L1, L2, and L3 on RT, $F_{(1, 32)} = 10.5$, $P < 0.001$, $\eta_p^2 = 0.279$; $F_{(1, 32)} = 2.89$, $P < 0.05$, $\eta_p^2 = 0.082$; $F_{(1, 32)} = 4.4$, $P < 0.05$, $\eta_p^2 = 0.12$; $F_{(1, 32)} = 0.1$, $P > 0.1$, $\eta_p^2 = 0.003$.

the effects of H1, H2, H3, $P > 0.1$, 95% CI -7.7 , 10.5 ($F_{(1, 32)} = 1.1$, $P = 0.31$). For the effects of L1, L2, L3, $F_{(1, 32)} = 2.89$, $P < 0.05$, 95% CI 1.8 , 11.7 , $F_{(1, 32)} = 4.4$, $P < 0.05$, 95% CI -9.1 , 4.4 , $F_{(1, 32)} = 0.1$, $P > 0.1$, 95% CI -5.8 , 5.4 . ANOVA revealed significant effects of H1, $F_{(2, 64)} = 10.5$, $P < 0.001$, $\eta_p^2 = 0.279$.

Imaging Data

Reward-based attentional capture in the visual cortex

We conducted a series of planned comparisons to test the effects of H1, L1, L2, and L3 on RT, $F_{(1, 32)} = 10.5$, $P < 0.001$, $\eta_p^2 = 0.279$; $F_{(1, 32)} = 2.89$, $P < 0.05$, $\eta_p^2 = 0.082$; $F_{(1, 32)} = 4.4$, $P < 0.05$, $\eta_p^2 = 0.12$; $F_{(1, 32)} = 0.1$, $P > 0.1$, $\eta_p^2 = 0.003$. We also conducted a series of planned comparisons to test the effects of H1, L1, L2, and L3 on RT, $F_{(1, 32)} = 10.5$, $P < 0.001$, $\eta_p^2 = 0.279$; $F_{(1, 32)} = 2.89$, $P < 0.05$, $\eta_p^2 = 0.082$; $F_{(1, 32)} = 4.4$, $P < 0.05$, $\eta_p^2 = 0.12$; $F_{(1, 32)} = 0.1$, $P > 0.1$, $\eta_p^2 = 0.003$.

ANOVA (L1, L2, L3)

$F(2, 32) = 1.99, p > 0.1, \eta_p^2 = 0.213$

$F(1, 16) = 4.32, P = 0.054, \eta_p^2 = 0.213$

L3. $F(2, 32) = 4.05, P < 0.05, \eta_p^2 = 0.202$. B

H1 H3, $P < 0.05$, 95% CI 0.0, 0.8 .

A H2

H1 H3, $P > 0.1$, 95% CI -0.6, 0.1 -0.2, 0.5 ,

$F(1, 16) = 7.18, P < 0.05, \eta_p^2 = 0.310$

H3. $F(1, 16) = 7.18, P < 0.05, \eta_p^2 = 0.310$

H1 L1, $t(16) = 3.84, P < 0.01$, 95% CI 0.2, 0.8 ,

H2 L2

H3 L3,

AI. The VS was significantly correlated with the FC strength between the AI and VS ($r = -0.29, P > 0.1$) in the pre-learning session (Figure 6A). In the post-learning session, the correlation was no longer significant ($r = -0.00, P > 0.1$) (Figure 6B). The difference in FC strength between the two sessions was significantly correlated with the RT difference between HI and LI conditions ($r = 0.63, P < 0.01$) in the left hemisphere and ($r = 0.53, P < 0.05$) in the right hemisphere (Figure 6C). All the FC strengths were within $\pm 3SD$ of the group mean.

Learning-induced changes in spontaneous brain connectivity

For the left hemisphere, the FC strength between the AI and VS was significantly correlated with the RT difference between HI and LI conditions in the pre-learning session ($r = -0.29, P > 0.1$) (Figure 6A). In the post-learning session, the correlation was no longer significant ($r = -0.00, P > 0.1$) (Figure 6B). The difference in FC strength between the two sessions was significantly correlated with the RT difference between HI and LI conditions ($r = 0.63, P < 0.01$) in the left hemisphere and ($r = 0.53, P < 0.05$) in the right hemisphere (Figure 6C). All the FC strengths were within $\pm 3SD$ of the group mean.

DISCUSSION

In this fMRI study, we investigated the learning-induced changes in spontaneous brain connectivity between the AI and VS in the pre-learning session, post-learning session, and the difference between the two sessions as a function of the RT difference between HI and LI conditions. We found that the FC strength between the AI and VS was significantly correlated with the RT difference between HI and LI conditions in the pre-learning session ($r = -0.29, P > 0.1$) (Figure 6A). In the post-learning session, the correlation was no longer significant ($r = -0.00, P > 0.1$) (Figure 6B). The difference in FC strength between the two sessions was significantly correlated with the RT difference between HI and LI conditions ($r = 0.63, P < 0.01$) in the left hemisphere and ($r = 0.53, P < 0.05$) in the right hemisphere (Figure 6C). All the FC strengths were within $\pm 3SD$ of the group mean.

Reward Breaks Through Center-Surround Inhibition in Visual Cortex

The results of the present study suggest that the learning-induced changes in spontaneous brain connectivity between the AI and VS are related to the reward breaks through center-surround inhibition in the visual cortex. The learning-induced changes in spontaneous brain connectivity between the AI and VS are related to the reward breaks through center-surround inhibition in the visual cortex. The learning-induced changes in spontaneous brain connectivity between the AI and VS are related to the reward breaks through center-surround inhibition in the visual cortex.

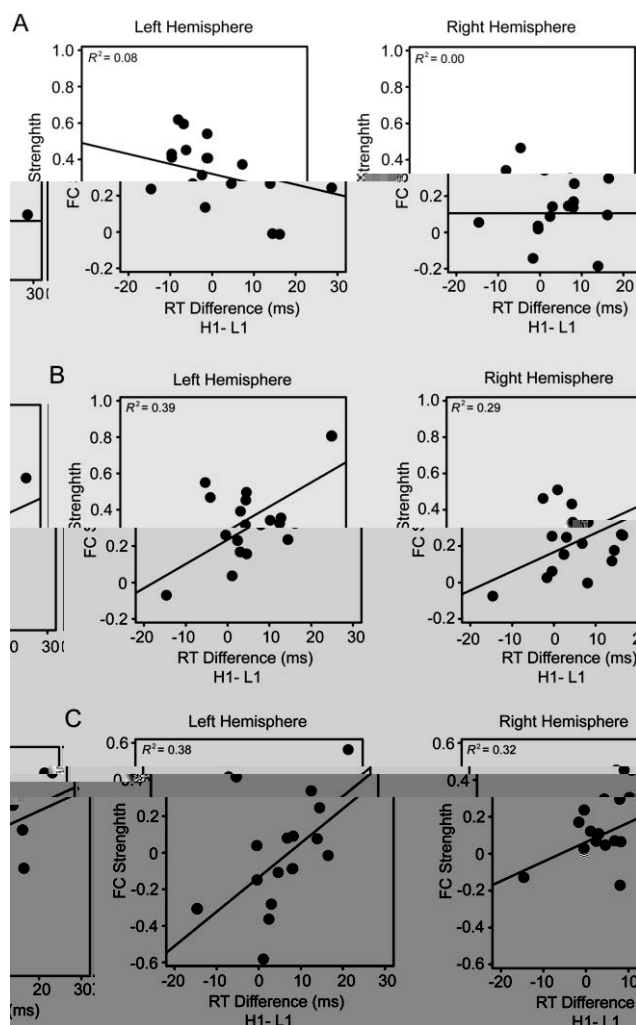


Figure 6.

Results of the resting-state fMRI. Scatter plots (with best-fitting regression lines) illustrates the FC strength between the AI and the VS in the pre-learning session (A), post-learning session (B), and the difference in FC strength between the two sessions (C) as a function of the RT difference between HI and LI conditions. Note that for both the behavioral interference effect and the FC strength, all of the individual observations were within $\pm 3SD$ of the group mean.

The results of the present study suggest that the learning-induced changes in spontaneous brain connectivity between the AI and VS are related to the reward breaks through center-surround inhibition in the visual cortex. The learning-induced changes in spontaneous brain connectivity between the AI and VS are related to the reward breaks through center-surround inhibition in the visual cortex. The learning-induced changes in spontaneous brain connectivity between the AI and VS are related to the reward breaks through center-surround inhibition in the visual cortex.

... (0.9°) ... (2.1°–4.5°). The ... (1.54°) ... (0.9°) ... (2.1°). H ... (1.6°–4°). T ... D ... B ... 2009; H ... 2006, ... G ... A ... C ... 2005; W ... 2013, ... W ... I ... W ... 2014. G ... C ... T ... 2003, ... 2.1° ... W ... 2014. I ... ($\geq 1.6^\circ$) ... MRI ... RT ... H1 ... H2 ... H3. M ... B ... RT ... H1 ... (H2, H3, L1, L2, L3), $P < 0.05$, ... RT ... ($e = 1$... $P = 0.08$, ... RT ... H3 ... L1). T ... W ... 2014, ... (H1) ... A ... W ... 2014. I ... M ... 2004; S ... 2013. I ... RT ... H1 ... H2 ... H3 ... (1.35°

... ($\geq 2.15^\circ$) ... RT ... H ... 2006; 2009, ... (... 1.6°–4°). T ... D ... B ... 2009; H ... 2006, ... G ... A ... C ... 2005; W ... 2013, ... W ... I ... W ... 2014. T ... G ... 2014. T ... Ge ... 2012. I ... Ge ... 2014; S ... 2015. G ... Ge ... 2014, ... (H3, H2) ... (H1). I ... H1 ... H2 ... H3 ... AI As the Source of Reward-based Salience in No-Reward Context ... P ... I ... H ... 2010

... effect of the ... - ...
... (MFN) ...
... (ACC). The ... ACC ...
... effect, ...
... ACC.
Here, the MFN ...
... ACC ...
... Ge ... W ...
2002; ... 2011 ...
I ...
... Ge ...
... AI ...
... DCM ... (e ...) ...
... AI IFG/IPS.

AI ...
... / ... C ... , 2009; See ... , 2007; U ... , 2015 .
C ... AI ...
... Lee ... S ... , 2013; Pe ... E ...
... , 2010 ... C ... , 2012;
D ... , 2005 . The ... AI ...
... See ... , 2005 . The ... AI ...
... AI ...
... A ... , 2012; U ... , 2015 .

I ... AI ...

TPJ (H2+H3) effect AI. CONCLUSION. ACKNOWLEDGMENTS. Te D. X. D. S. e L f MRI M D M W f e e e f . T e N B Re e P (973 P : 2015CB856400) f e M f S e e Te - f C . Te e e e f e e .

REFERENCES

A e GA, C P (2005): I e e e e e f e - e e f e e e e e . P 16:637 643.
 A e BA (2013): A e - e e e e f e e e . J V 13:7 7.
 A e BA, S (2013): Pe e e f e - e e e . J E P H Pe e Pe f 39:6 9.
 A e BA, L e PA, S (2011): V e - e e e . P N A S U S A 108:10367 10371.
 A e BA, L e PA, S (2014): V e - e e e - e . B Re 1587:88 96.
 A e JT, Ne e K, J B, V f e W (2013): D e e e e e e e f MRI e e e . Ne 77:1174 1186.
 A E, Be AV, Tee e J (2012): T - e e e e . A f e e e e e . T e C S 16:437 443.
 Be e KC, R TE (1998): W e e e f e e e e e ? B Re Re 28:309 369.
 Be e CN, T JK, S e f e MA, He e HJ, H f JM (2009): T e e e - e e f e f f e e e f e e e . C e e C e 19:982 991.
 C W, C e T, S R, K J, L CR, Me V (2015): C e e e f e - e e e e e e e e . C e e C e , 046.
 C e AR, A e SV, L CE, C LT, Re e J, S e MJ, P e DL, S GL, C e M (2010): Re e e e f e e e e e e e e e . A Ne 67: 365 375.
 C LJ, T, K MW, S f e AG (2013): De e e e f e e e e e . F e e e e e e e e e e e e e . C e e C e 23:739 749.
 C e L, Pe e A, S e e E, De L e C (2013): Re e e e e e . V Re 85:58 72.
 C e T, M e L, S e K, K J, R S, Me V (2015): R e f e e e e e e e e e e e e . E J Ne 41:164 274.
 C JM, P S, Pe L (2012): I f e e e e e e e e e e e e . Ne e 59:1912 1923.
 C e M, S GL (2002): C f e - e e e e e e e e e . N Re Ne 3: 201 215.
 C e M, K e JM, O e JM, M A MP, S GL (2000): V e e e e f e e e e e e e . N Ne 3:292 297.
 C e D (2005): C e e e e e e e e e e e . A e e e e L f e M e e e . T Q Me P 1:42 45.
 C AD (2009): H f e e ? T e e e e e e . N Re Ne 10:59 70.
 C F, T JK (2003): T e e e e e e f e e e . P e e e f e e e e e e e . V Re 43:205 219.

D... KM, K... NH, G... TM, D... RJ (2005): Ne... - -
969 980.

De... e R, D... J (1995): Ne... e... f... e... -
... A... Re... 18:193 222.

D... J, C... AP, M... DJ, D... KD (2000): A... -
... e... f... e... f... e... e...
... N... 3:277 283.

F... CL, Re... RW, J... JC (1992): I... e... e...
... e... e... e... J E
P... :H... Pe... Pe... 18:103047.

F... KJ, H... L, Pe... W (2003): D... e... e...
... Ne... 19:1273 1302.

F... KJ, Pe... WD, G... DE (2005): C... e... e...
... Ne... 25:661 667.

Ge... WJ, W... AR (2002): T... e... f... e...
... e... f... e... e... S... e... 295:
2279 2282.

Ge... JJ (2014): A... e... e... f... e... e...
... C... D... P... S... 23:147 153.

H... e SN, K... B (2010): T... e... :L... e... e...
... Ne... 35:
4 26.

H... e C, Pee... MV (2015): Ne... e... f... e... e...
... Ne... 85:512 518.

H... e C, C... L, Tee... J (2010): Re... e... e... e...
... e... e... e... J Ne... 30:
11096 11103.

H... f... JM, B... e CN, L... SJ, T... JK, He... e HJ, S... e...
MA (2006): D... e... e... e... e... f... e... -
... e... e... f... f... e... P...
N... A... S... U S A 103:1053 1058.

K... e JM, A... RA, A... e SV, S... GL, C... e... M
(2005): A... e... -e... f... e... e... e... e... -
... f... e... -e... e... f... e...
... J Ne... 25:4593 4604.

Ke... RM, B... e CN E... T, W... ff (2011): T... e...
... e... f... e... e... e... e...
... e... e... J Ne... 31:9752 9759.

Lee J, S... e S (2013): T... e... f... e... e... f... e...
... e... e... e... e... J Ne... 33:
10625 10633.

Le... MI, S... e MN (1999): E... f... e... e... e... -
... e... e... e... f... e... e... e... e... e... f... e...
... f... e... e... Ne... 24:415 425.

Lee... MD, C... WA (2009) e... e... eI(31:9752 e... e)-325... II(31:97...)-60 e... ()-35TD fMRI T*(e... e... e)-:-35TD7* -

- Schultz, W., Glimcher, T. C., & Portman, C. M. (2013). A neural mechanism of reward-based attention. *Journal of Neuroscience*, 33(11), 3913-3924. doi:10.1523/JNEUROSCI.4111-12.2013
- Seidemann, K. E., Pezawas, W. D., Doherty, J. M., & Fiez, J. A. (2009). Behavioral and neural mechanisms of reward-based attention. *Neuron*, 64(4), 1004-1017. doi:10.1016/j.neuron.2009.08.011
- Tee, J. (1991). Cerebral mechanisms of attention. *Psychological Review*, 98(2), 184-193. doi:10.1037/0033-2909.98.2.184
- Tee, J. (1992). Perceptual and attentional mechanisms of attention. *Psychological Review*, 99(4), 599-606. doi:10.1037/0033-2909.99.4.599
- Uchida, N. (2015). Selective attention and the neural mechanisms of attention. *Neuron*, 86(1), 16-55. doi:10.1016/j.neuron.2015.02.021
- Vogel, S., Weibull, R., & Theeuwes, J. (2009). What is the neural mechanism of attention? *Journal of Cognitive Neuroscience*, 21(3), 30-41. doi:10.1162/jocn.2009.2130
- Vogel, S., Weibull, R., Doherty, J. M., & Fiez, J. A. (2012). Developmental changes in the neural mechanisms of attention. *Journal of Neuroscience*, 32(32), 10637-10648. doi:10.1523/JNEUROSCI.2511-12.2012
- Wang, L., & Huk, D. J. (2013). The neural mechanisms of reward-based attention. *Journal of Neuroscience*, 33(11), 3913-3924. doi:10.1523/JNEUROSCI.4111-12.2013
- Wang, L., Doherty, J. M., & Fiez, J. A. (2014). Reward-based attention and the neural mechanisms of attention. *Journal of Neuroscience*, 34(14), 4412-4422. doi:10.1523/JNEUROSCI.4111-12.2013
- Wang, P., & Glimcher, T. C. (2013). A neural mechanism of reward-based attention. *Journal of Neuroscience*, 33(11), 3913-3924. doi:10.1523/JNEUROSCI.4111-12.2013
- Wang, P., & Glimcher, T. C. (2010). DPARSF: A MATLAB Toolbox for Dynamic Programming-based Analysis of fMRI Data. *Neuroinformatics*, 8(1), 4-13. doi:10.1007/s12028-010-9101-1
- Wang, S. J., & J. (1984). A neural mechanism of reward-based attention. *Journal of Experimental Psychology: Human Perception and Performance*, 10(6), 601-621. doi:10.1037/0096-1467.10.6.601
- Wang, S. J., & J. (1990). A neural mechanism of reward-based attention. *Journal of Experimental Psychology: Human Perception and Performance*, 16(1), 121-134. doi:10.1037/0096-1467.16.1.121
- Wang, R., & Wang, X. (2011). Reward-based attention and the neural mechanisms of attention. *PLoS ONE*, 6(12), e29633. doi:10.1371/journal.pone.0029633